Supplementary figures

Supplementary figure 1

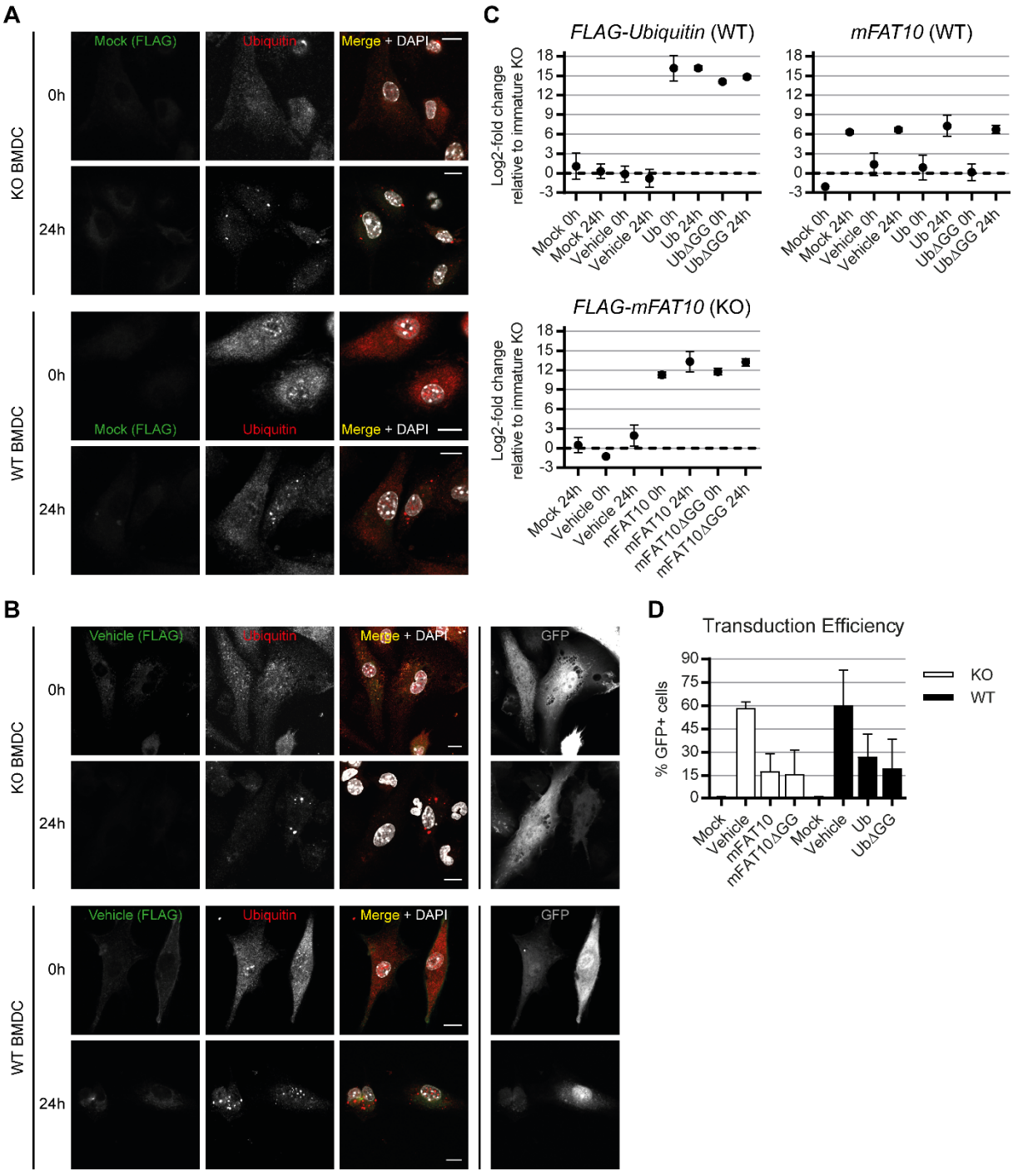

Fig. S1. DALIS formation is not influenced in mock- and vehicle-transduced BMDCs. Bone marrow-derived DCs (BMDCs) were generated from *FAT10*-deficient (KO BMDC) and -proficient (WT BMDC) mice. The progenitor cells were transduced on day 3 of culture and immature BMDCs stimulated or not on day 10 using 400 U/mL TNF and 200 U/mL IFN-γ.

(A, B) KO and WT BMDCs were mock-transduced (A) and were transduced with vehicle lentiviruses that only express GFP (B). Four hours prior to sample preparation for confocal microscopy, 5 µM MG132 was added to mock- and vehicle-transduced BMDCs. Immature (0 h) and mature (24 h) transduced BMDCs were stained with anti-ubiquitin and anti-FLAG antibodies. Nuclei were counterstained using DAPI and images were acquired on an LSM880 confocal microscope at 63x magnification. GFP signals were excluded from the merged images in (B) for clarity. Representative images of three to four independent experiments are shown. The scale bar is 10 µm. (C) Homologous expression of the *ubiquitin* transgene was determined using *IRES*-specific primers to distinguish the expression from endogenous *ubiquitin*. For the expression level of the *mFAT10* transgene and endogenous *mFAT10*, *mFAT10*-specific primers were used. Expression levels were normalised to m*ACTB* and are depicted as log2-fold change relative to immature mock-transduced KO BMDCs (represented as the dotted line in all three graphs). (D) One day prior to stimulation the transduction efficiency was determined by measuring the percentage of GFP^+ cells using flow cytometry. Results of two to four independent experiments are shown as mean ± SD (C, D).

Supplementary figure 2

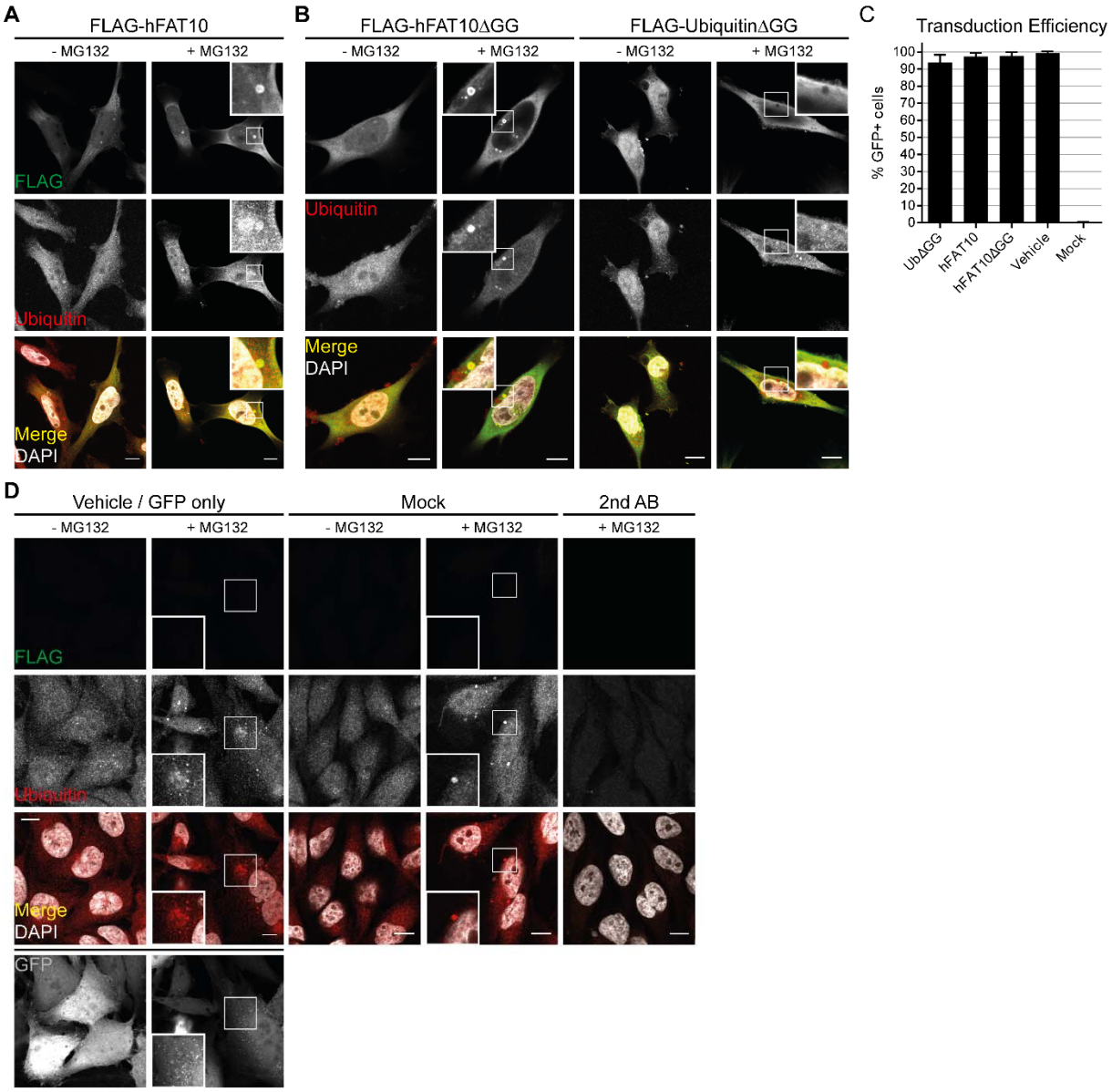

Fig. S2. FAT10 localises to aggresomes independently of conjugation. (A, B) HeLa cells were transduced using lentiviral vectors encoding human FLAG-hFAT10 (A) and the non-conjugatable forms of hFAT10 and ubiquitin (FLAG-hFAT10ΔGG, FLAG-ubiquitinΔGG) (B). (C) On day 3 of culture prior to seeding for confocal microscopy, the transduction efficiency was determined by flow cytometric detection of the GFP-reporter expressed by the lentiviruses. The percentage of GFP^+ cells is given as mean ± SD. (D) Control cells were not transduced (Mock) or transduced with lentiviruses expressing only GFP (vehicle). Aggresome formation was induced on day 4 by proteasome inhibition using 10 μM MG132 (+MG132) for 6 h. As a

control in A, B, and C, cells were left untreated to exclude overexpression artefacts (-MG132). After fixation, samples were stained for ubiquitin and FLAG-tagged proteins. Control samples were stained with secondary antibodies only (D, right column 2nd AB). Nuclei were counterstained with DAPI. Images were acquired using a LSM880 confocal microscope at 63x magnification. Inlets highlight aggresomes of interest. For clarity, the GFP channel was excluded from the merged images in (D). Representative images of three independent experiments are shown. Scale bar is 10 µm.

Supplementary figure 2 shows localisation of FAT10 to aggresomes independent of conjugation and the dependence of ubiquitin on conjugation for aggresome targeting, which has been reported before (Kalveram et al., 2008; Ouyang et al., 2012). Notably, three to four days after transduction with lentiviruses encoding FLAG-tagged ubiquitin increased cell death was observed that was likely due to the overexpression of ubiquitin as reported before (Crinelli et al., 2008). Therefore, it was impossible to acquire images for this construct.

Supplementary figure 3

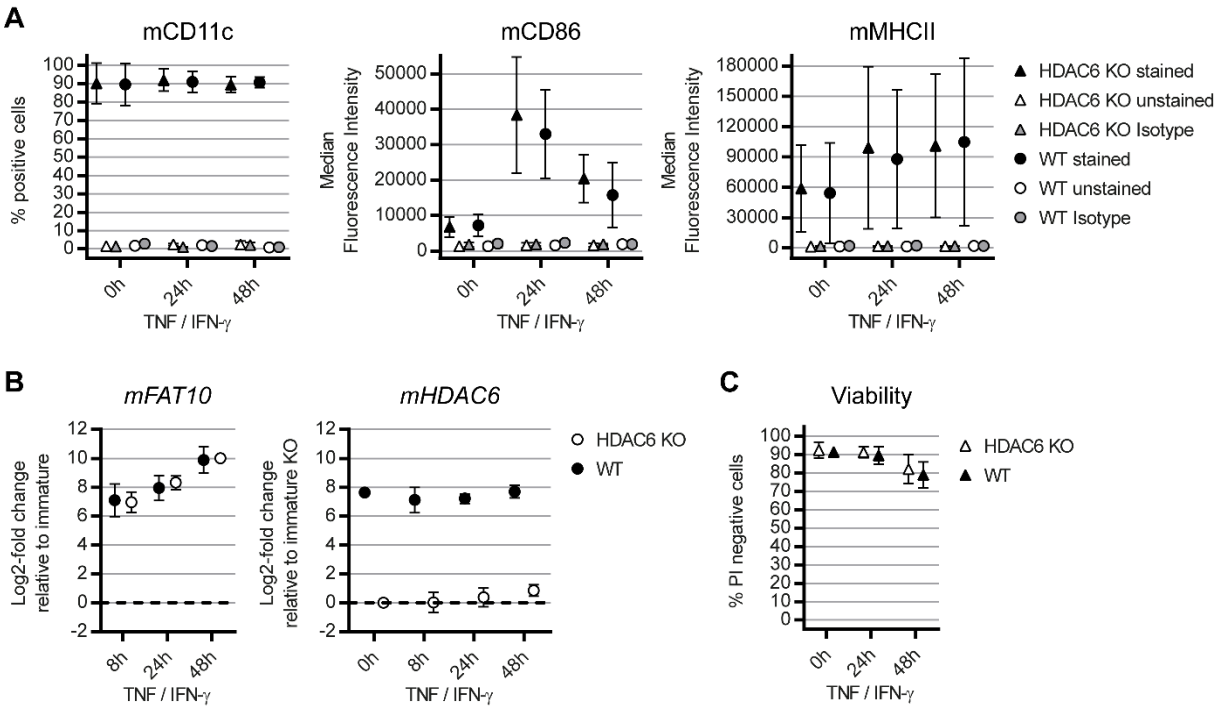

Fig. S3. Analysis of the maturation of *HDAC6*-deficient and -proficient DCs. *HDAC6*-deficient (HDAC6 KO) and -proficient (WT) BMDCs were generated and maturation was induced using 400 U/mL TNF and 200 U/mL IFN-γ. At the indicated time points BMDCs were analysed by flow cytometry (A, C) and qPCR (B). (A) The percentage of $CD11c^+$ BMDCs and upregulation of CD86 and MHC class II surface expression on BMDCs upon maturation by cytokines was determined. (B) Expression level of *mHDAC6* and *mFAT10* were determined by qPCR and normalised to *mHPRT* and *mACTB*. *mACTB* was excluded from samples at 48 h of maturation due to unstable expression. *mFAT10* expression is shown relative to immature HDAC6 KO or WT BMDCs (depicted as dotted line) to see up-regulation of *mFAT10* upon maturation in BMDCs from both genotypes. *mHDAC6* expression is depicted relative to immature HDAC6 KO BMDCs (shown as dotted line) to see the expression level of *mHDAC6* in immature WT BMDCs. (C) The viability of BMDCs was assessed at indicated time points using propidium iodide. Results are summarised from three independent experiments and depicted as mean ± SD.

Supplementary figure 4

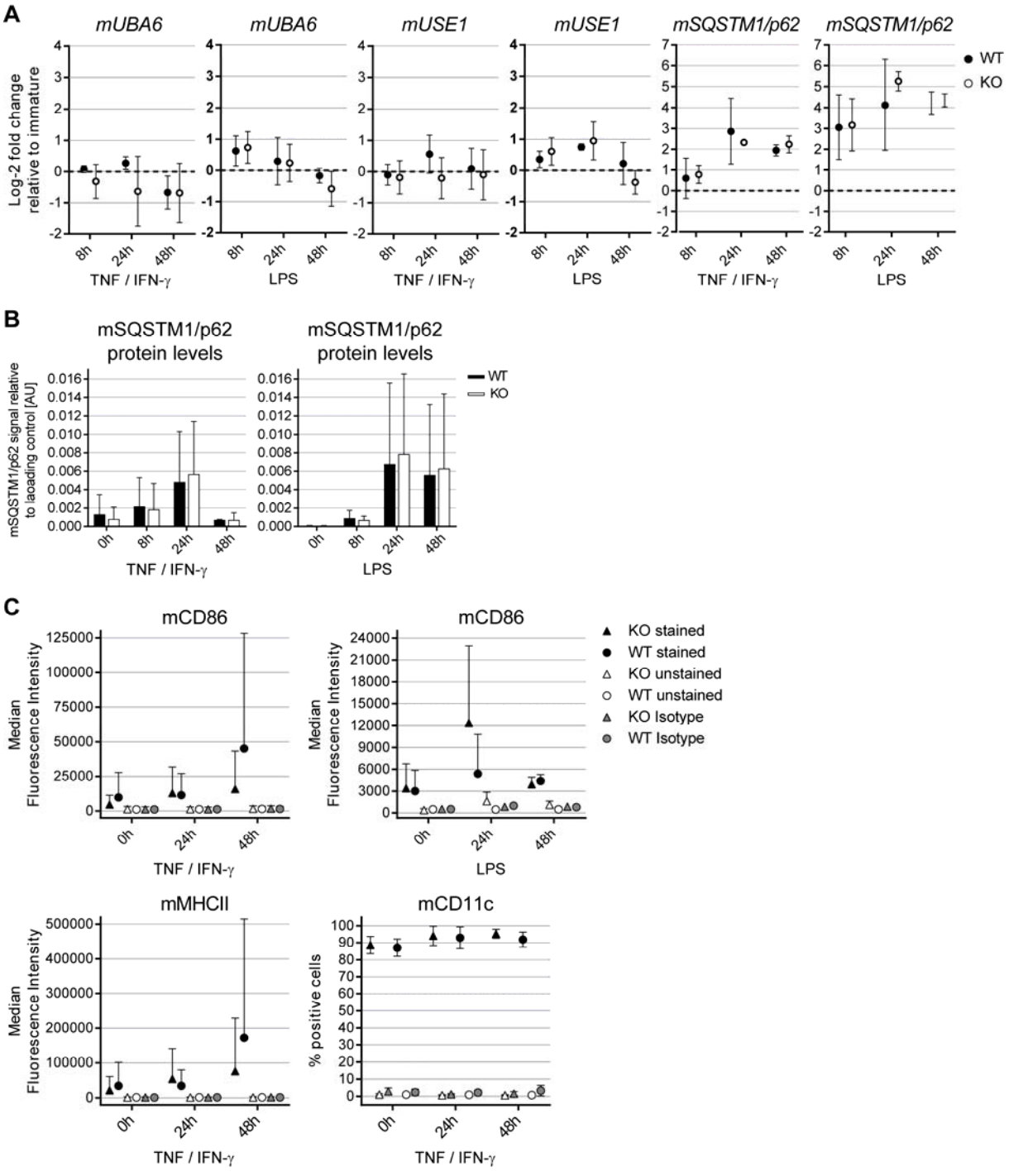

Fig. S4. Expression profile of FAT10-related proteins in BMDCs and maturation characteristics of BMDCs. BMDCs were generated from *FAT10*-deficient (KO) and -proficient (WT) mice. On day 10 of culture, maturation was induced by 1 µg/mL LPS or 400 U/mL TNF and 200 U/mL IFN-γ. BMDCs were analysed at the indicated time points. (A) Expression levels of *mUBA6*, *mUSE1*, and *mSQSTM1/p62* determined by qPCR in cytokine- or

LPS-matured BMDCs. Expression levels were normalised to *mHPRT* and *mACTB* and depicted as log2-fold change relative to immature KO or WT BMDCs (indicated as dotted line). Results of two to four experiments are shown. (B) mSQSTM1/p62 protein levels in BMDCs were quantified from Western blots and normalised to the loading control. β-actin was used as loading control. Results of two to three experiments are shown. (C) Cell surface staining of mCD86, mMHC class II, and mCD11c on cytokine- and LPS-matured BMDCs at the indicated time points. Summary of two (LPS) and four to five (TNF / IFN-γ) experiments. Results in A-C show the mean ± SD.

Table S1: Primer pairs used to detect endogenously expressed and overexpressed mRNAs.

mRNA	Forward (5′ to 3′)	Reverse (5′ to 3′)
(HUMAN) *FAT10*	AATGACCTTTGATGCCAACC	GCCGTAATCTGCCATCATCT
(HUMAN) *GAPDH*	GAAGGTGAAGGTCGGAGT	GAAGATGGTGATGGGATTTC
(MOUSE) *FAT10*	GCTTCTGTCCGCACCTGTGTTGT	TGGGGCTTGAGGATTTTGGAGTCT
(MOUSE) *UBA6*	GTTCCTTCTCCCACAAACCT	TTGCCAAAACAAACTGCCAT
(MOUSE) *USE1*	AAACTGATGACAACGGGCAA	TGCTGTCTCCTGGATGTCTT
(MOUSE) *p62*	GCTGCCCTATACCCACATCT	CGCCTTCATCCGAGAAA
(MOUSE) *HDAC6*	TCAGCACAATCTTATGGATGG	CCACGATGAGAACCCTCTG
(MOUSE) *ACTB*	GACCTCTATGCCAACACAGT	ACTCATCGTACTCCTGCTTG
(MOUSE) *HPRT*	CCAGCAGGTCAGCAAAGAACTTA	TGGACAGGACTGAAAGACTTG
FLAG-X-IRES	GATCCGACTACAAAGACCATGAC	AACATATAGACAAACGCACACC

References

Crinelli, R., Bianchi, M., Menotta, M., Carloni, E., Giacomini, E., Pennati, M. and Magnani, M. (2008). Ubiquitin over-expression promotes E6AP autodegradation and reactivation of the p53/MDM2 pathway in HeLa cells. *Mol. Cell. Biochem.* **318**, 129–145.

Kalveram, B., Schmidtke, G. and Groettrup, M. (2008). The ubiquitin-like modifier FAT10 interacts with HDAC6 and localizes to aggresomes under proteasome inhibition. *J. Cell Sci.* **121**, 4079–4088.

Ouyang, H., Ali, Y. O., Ravichandran, M., Dong, A., Qiu, W., MacKenzie, F., Dhe-Paganon, S., Arrowsmith, C. H. and Zhai, R. G. (2012). Protein aggregates are recruited to aggresome by histone deacetylase 6 via unanchored ubiquitin C termini. *J. Biol. Chem.* **287**, 2317–2327.